

Final Concept and Design

EML 4551C – Senior Design – Fall 2011 Deliverable

Group # 1

Joseph Chason, Donald Hayes II, Zachary Johnson, Sarah Napier

Air Bearing Upgrade for the Split-Hopkinson Pressure Bar Experiment

Department of Mechanical Engineering, Florida State University, Tallahassee, FL

Project Sponsor

Eglin Air Force Research Laboratory



Project Advisor

Dr. Kalu, PhD

Department of Mechanical Engineering

Erica Cosmutto, ME Graduate Student

Reviewed by Advisor:

Table of Contents

Table of Figures	4
Table of Tables	5
Table of Equations	6
Executive Summary –	8
Introduction –	9
Needs Assessment –	10
Client Requirements –	10
Problem Statement	10
Objectives	10
Product Specifications –	11
Background Research –	11
SHPB –	13
Air Bushings and Supply –	14
Air Bushings -	14
Air Supply -	15
Strain Gauges -	15
Project Plan –	17
Concept Design –	17
Striker Bar Mechanism –	18
Incident and Transmitted Bars/ Air Bushings –	20
Base –	22
Data Acquisition/ Air Supply –	23
Strain Gauges –	24
Momentum Trap –	26
Bushing Alignment –	27
Decision Matrix –	29
Final Design –	30
Cost Analysis –	32
Analysis –	33

Striker Velocity Analysis/Solenoid optimization –.....	38
Optimization and Analysis of the Solenoid.....	41
Finite Element Analysis (FEM) –	43
Comsol Intro-.....	43
Comsol analysis –.....	44
Environment and Safety –.....	47
Conclusion –	47
References –.....	49
Appendix A –.....	51
Complete Cost analysis	51
Pro Engineer Models –.....	52

Table of Figures

Figure 1 -15

Figure 2 -16

Figure 3 -16

Figure 4 -18

Figure 5 -18

Figure 6 -20

Figure 7 -20

Figure 8 -22

Figure 9 -22

Figure 10 -24

Figure 11 -24

Figure 12 -25

Figure 13 -25

Figure 14 -28

Figure 15 -29

Figure 16 -29

Figure 17 -29

Figure 18 -29

Figure 19 -37

Figure 20 -40

Figure 21 -43

Figure 22 -44

Table of Tables

Table 1 -17

Table 2 -19

Table 3 -19

Table 4 -20

Table 5 -23

Table 6 -25

Table 7 -26

Table of Equations

$\sigma = F/A$ Eqn. 1.....	33
$\varepsilon = (L_i - L_o) / L_o$ Eqn. 2.....	33
$\sigma = E * \varepsilon$ Eqn. 3.....	33
$GF = [(R_i - R_g) / R_g] / \varepsilon$ Eqn. 4.....	34
$\varepsilon = [(R_i - R_g) / R_g] / GF$ Eqn. 5.....	34
$R_g = (R_2 / R_1) * R_3$ Eqn. 6.....	34
$V_g = [(R_g / \{ R_3 + R_g \}) - (R_2 / \{ R_1 - R_2 \})] * V_a$ Eqn. 7.....	34
$d\varepsilon_{avg} / dt = (C_b / L_s) * (\varepsilon_I - \varepsilon_R - \varepsilon_T)$ Eqn. 8.....	35
$\varepsilon_s = (C_b / L_s) * \int_0^t [(\varepsilon_I - \varepsilon_R - \varepsilon_T) * dt]$ Eqn. 9.....	35
$\sigma_1 = (A_B / A_s) * E_B * (\varepsilon_I + \varepsilon_R)$ Eqn. 10.....	35
$\sigma_2 = (A_B / A_s) * E_T$ Eqn. 11.....	36
$\sigma_{avg} = 0.5 * (\sigma_1 + \sigma_2)$ Eqn. 12.....	36
$E_I = 0.5 * A_B * C_B * E_B * T * \varepsilon_I^2$ Eqn. 13.....	36
$E_I = 0.5 * A_B * C_B * E_B * T * \varepsilon_R^2$ Eqn. 14.....	36
$E_I = 0.5 * A_B * C_B * E_B * T * \varepsilon_T^2$ Eqn. 15.....	36
$\delta S_E = E_I - E_R - E_T$ Eqn. 16.....	36
$K_I = 0.5 * \rho_B * A_B * C_B^3 * T * \varepsilon_I^2$ Eqn. 17.....	36
$K_R = 0.5 * \rho_B * A_B * C_B^3 * T * \varepsilon_R^2$ Eqn. 18.....	36
$K_T = 0.5 * \rho_B * A_B * C_B^3 * T * \varepsilon_T^2$ Eqn. 19.....	36
$\delta K_E = E_I - E_R - E_T$ Eqn. 20.....	36
$E_s = 2 * \delta K_E = 2 * \delta S_E$ Eqn. 21.....	36
$GF = [(R_i - R_g) / R_g] / \varepsilon$ Eqn. 22.....	37
$\varepsilon = [(R_i - R_g) / R_g] / GF$ Eqn. 23.....	37
$R_x = (R_2 / R_1) * R_3$ Eqn. 24.....	38
$V_g = [(R_g / \{ R_3 + R_x \}) - (R_2 / \{ R_1 - R_2 \})] * V_a$ Eqn. 25.....	38
Eqn. 26.....	39
Eqn. 27.....	39
Eqn. 28.....	39
Eqn. 29.....	39
Eqn. 30.....	39
Eqn. 31.....	39
Eqn. 32.....	39
Eqn. 33.....	39
Eqn. 34.....	39
Eqn. 35.....	39
Eqn. 36.....	40
$\sigma_{y\text{infinite}} = \frac{\sigma_y}{2}$. Eqn. 37.....	40
Eqn. 38.....	40

Eqn. 39 40
 Eqn. 40 40
 Eqn. 41 40
 Eqn. 42 40
 Eqn. 43 40

$$\rho \cdot A \cdot \frac{d^2}{dt^2} T - \frac{d}{dx} \left[E \cdot A \cdot \left(\frac{d}{dx} u \right) \right] - f(x, t) = 0 \quad \text{Eqn. 44} \dots\dots\dots 43$$

$$\int \left[w \cdot \rho \cdot A \cdot \frac{d^2}{dt^2} T - w \cdot \frac{d}{dx} \left[E \cdot A \cdot \left(\frac{d}{dx} u \right) \right] - w f(x, t) \right] dx = 0$$

Eqn. 45 43
 Eqn. 46 43
 Eqn. 47 Eqn. 48 Eqn. 49 44

Executive Summary –

The Senior Design Project, The Air Bearing Upgrade for the Split Hopkinson Pressure Bar (SHPB) which is designated to Group 1 is sponsored by Dr. Joel House at the Eglin Air Force Research Laboratory. The task of the group is to upgrade the current air bearings that are used on the 0.625” Split Hopkinson Pressure Bar at Eglin. To decide which air bearings would best suit the SHPB, research was done from a few companies, and factors such as cost, availability, and efficiency were explored upon making a decision.

In addition to selecting the air bearings for the Eglin SHPB, the group was asked to make a smaller prototype at the FAMU/FSU College of Engineering that would represent the larger one at the Eglin Research Lab. Decisions were made based on what size bars and bushings would be best for the prototype in order to achieve the desired goals. Other decisions that had to be made included what kind of mechanism would be best for striking the incident bar and if it would reach the necessary velocity to deform a test specimen. Another issue was how the SHPB apparatus could be mounted so that it would remain sturdy during operation. Also, determining how to precisely align the bushings so that the incident and transmitted bars would slide properly became a significant factor in how the device would work. An air supply system is necessary as the air bushings must receive the correct amount and pressure of air to function correctly. The kinds of strain gauges that would be best for mounting onto the bars and how to wire them brought forth another question. A momentum trap was needed to bring the SHPB device to rest. In order to receive data from the experiment, the best kind of data acquisition system will be implemented into the prototype. With the help of the assigned sponsor and building the prototype

in the spring of 2012, more knowledge will be gained on how to operate a fully functioning Split Hopkinson Pressure Bar.

Introduction –

The split – Hopkinson pressure bar (SHPB) system is used to test the stresses and strains on various specimens in order to cause plastic deformation. The system begins with a striker bar mechanism that sets everything in motion. The striker bar is ejected out of a barrel with a constant velocity until it comes in contact with the incident bar. This contact begins a wave in the form of a square pulse that runs through the incident bar to the opposite end where the incident bar comes in contact with the specimen. At this point, the pulse splits in to, where one pulse returns to the front end of the incident bar while the other pulse goes through the specimen, causing it to plastically deform and then into the transmitted bar. The transmitted bar is then set in motion, in which case it is stopped by a momentum trap. Strain gauges are placed on both the incident and transmitted bars in the form of a Wheatstone bridge. A data acquisition system is attached to the strain gauges in order to plot the pulse going through the bars to see the trend in plastic deformation of the specimen.

Currently at Eglin AFRL, the SHPB system has ball bearings that the incident and transmitted bars move through, which do encounter friction that affects the performance of the system. It was the intention of this project to implement the use of air bushings to allow for an almost ideal situation with little to no friction. The following report contains the research, calculations and selection of components in order to generate a small-scale SHPB system by the end of the spring semester of 2012.

Needs Assessment –

Warhead design engineers and material scientists require mechanical property information under high deformation rates of loading on a wide variety of materials that have military significance. The most generally accepted technique for gathering such information is the SHPB experiment. The Air Force Research Laboratory's Damage Mechanisms Branch has operated such an experiment for approximately 30 years. The Damage Mechanisms Branch has a requirement to replace the current bearing system with a new air bearing design.

Client Requirements –

Problem Statement

The goal of this project is to upgrade the current bearing system located on the Split-Hopkinson Pressure Bar experiment in the Air Force Research Laboratory's Damage Mechanism Branch at Eglin AFB to a system utilizing near-frictionless air bearings.

Objectives

The most crucial objectives of this project are as follows:

1. Analyze the engineering challenge of upgrading the Eglin AFB SHPB to a physical architecture based on the use of air bearings.

2. Provide analysis of air bearing hardware cost, interface requirements, installation procedures and impact on the bar geometry.
3. Provide an assessment of strain gauge technology.
4. Develop a procedure to align the bars based on the new architecture.

Other objectives of the project are the acquisition of suitable bearings and related equipment, the installation of the new bearing system on the SHPB, and the initial testing of the SHPB.

Product Specifications –

The SHPB mechanism will consist of air bushings with an air supply, an incident bar, a transmitted bar, strain gauges and a mechanism to initially move the incident bar. The main idea of this project is to implement the main components of the experiment, mainly five-eighths inch diameter bars and corresponding air bushings, into a table top version to gain information for the AFRL.

Background Research –

In 1914, Bertram Hopkinson came up with a way to use a metal bar to test stress pulses. H.Kolsky, in 1949, used Hopkinson's idea and expanded upon it. He devised an experiment

using two collinear bars to measure stress and strain through a pressure wave, known today as the split-Hopkinson pressure bar experiment.

In this experiment, a specimen is placed between the two collinear bars, transmitted bar and the incident bar, that are placed in a certain number of bearings and are equipped with strain gauges placed on them at specific locations. A device at the opposite end of the incident bar is used to set the bar in motion, creating an incident wave. The bar forces into the specimen, which pushes the transmitted bar into a shock absorbing barrier. The incident wave that is generated goes through the incident bar to the specimen where it is split into two waves before it reaches the specimen. The transmitted wave goes through the specimen, plastically deforming it, while the reflected wave reflects from the specimen back through the incident bar. The stress and strain of the deformed specimen can be calculated using the information collected from the strain gauges.

The Split Hopkinson Pressure Bar, also called the Kolsky Bar is a device used to determine material properties such as stress-strain behavior. The setup consists of two metal bars, the incident bar and the transmitted bar, in which a material sample is placed in between. The bar diameter can vary in size. A bar diameter of 5/8 in. will be used at the Eglin Air Force Research Lab which is for the purpose of this senior design project. A stress wave is propagated and measured through the bar and the specimen. It is important that the bars are precisely aligned. This will be a critical task that must be conducted for the apparatus to work properly. The Split Hopkinson Pressure Bar device is always mounted onto a sturdy base. The bar setup at the Eglin Research Lab is mounted to an I-beam.

At certain locations along the Hopkinson bar are several air bearings. The project involves the upgrade of new air bearings to replace the current bearings on the bar at Eglin. The

air bearings provide a thin pressurized air film that is nearly frictionless in which the bars can easily move. There must be a tolerance between the bearing and the bar, so that the bar will not be hindered from moving. An air supply tube will distribute air to each bearing. The placement of the air bearings cannot interfere with the strain gauges. The spacing of the bearings and the gauges will be determined through analysis from both previous experiments and experiments that will be performed.

SHPB –

The Split Hopkinson Pressure Bar that will be used at the Eglin Air Force Research Lab is expected to have a diameter of 5/8 in. There is the possibility that the bar diameter will be slightly larger or smaller because of the air bushing sizes that are available at certain companies.

A diameter will be chosen by the group for the model that will be built at the FAMU-FSU College of Engineering. Some factors that will determine the selection of the diameter size for the mock-up include the material of the bar, the compatibility with air bearing bushing sizes, and the cost. Also, the length of the bar used in the model will be scaled down. The alignment of the bar is critical for obtaining accurate results. The bars will have to be interfaced to a support. The support used at Eglin is an I-beam. The support design that will be chosen for the model will be influenced by factors such as cost and strength.

Air Bushings and Supply -

Air Bushings -

Although the name of this project implies the use of air bearings, what will actually be used in the final design will be air bushings. An example of an air bearing is the surface of an air hockey table which allows for reduced friction while still permitting 3 degrees of freedom (2 linear and 1 rotational) to an object passing over its surface. In contrast, air bushings are used to restrict a rod's movement to linear motion along and rotational motion about the rod's lengthwise axis.

Given the bars in the final SHPB experimental model must maintain tight, co-linear tolerances while significantly reducing friction, air bushings will provide the better solution. There are multiple types of air bushings, and the bushing most suitable to this project must be determined. One of the main distinctions between types of air bushings is the method by which compressed air is supplied to the 'contact' surface between the bushing and rod. The most basic method is the placement of one or more small outlets in the contact surface. This method can be modified to include shallow channels in the contact surface which guide the compressed air away from the outlets in order to achieve a more uniform pressure distribution. The method which provides the most even pressure distribution involve the use of an air-permeable material, such as porous carbon, to distribute the compressed air along the contact surface. Whichever type of air bushing is chosen and implemented in the final design, a significant reduction in the friction between the bushings and rods should be achieved when compared to the contact friction inherent in the use of more traditional metal or ceramic ball bearings.

Air Supply -

Given that air bushings are to be used in the completion of this project, the method by which those bushings are to be supplied with compressed air must also be addressed. The main portion of the air supply system will be a compressor; the size and rating of which will be determined by the requirements of the bearings. Assuming that not all bushings are created equal, those which could be selected for the project will have differing requirements as to the pressure and quality of air they must be supplied in order to properly function. As an example, New Way Air Bearings produces an air bushing for 0.75 inch diameter rods. This bushing requires a flow rate of 7.0 to 9.60 Standard Cubic Feet per Hour (SCFH) while other bushings of the same type require flows between 2.25 and 37.8 SCFH. Also, because this bearing utilizes a porous contact surface, it requires air that has been dried and cleaned using first a general-purpose filter, followed by a coalescing filter, and a desiccant dryer. This level of air purification would require higher air quality control than is available on the average shop compressor. The implementation of a filter and drying system between the compressor and bushings will likely be required. If so, the choice of this system may affect the usefulness of the final design as much as the choices of compressor or bushings themselves.

Strain Gauges -

The strain gauge is a device used to measure the amount of deformation over the original length of a certain object after a force has been applied. The values for strain are usually less

than 0.005 and are displayed in micro-strain units. Strain can be measured for tensile or compressive loads. The strain will be measured in compression for the purpose of this experiment. A strain gauge works by converting mechanical motion into an electrical signal. The sensor responds to a change in capacitance, inductance, or resistance. In this experiment the strain gauge will respond to the change in resistance. The strain gauge must be connected to an electrical circuit which will be a Wheatstone bridge circuit for this case.

The strain gauges on the Split Hopkinson Pressure Bar measure the strain from the propagating wave. The strain gauges will be placed on the bars so that the waves do not overlap and cause disturbed signals. A factor for choosing the correct strain gauge is the degree of accuracy which will influence the results of the experiment.

Project Plan –

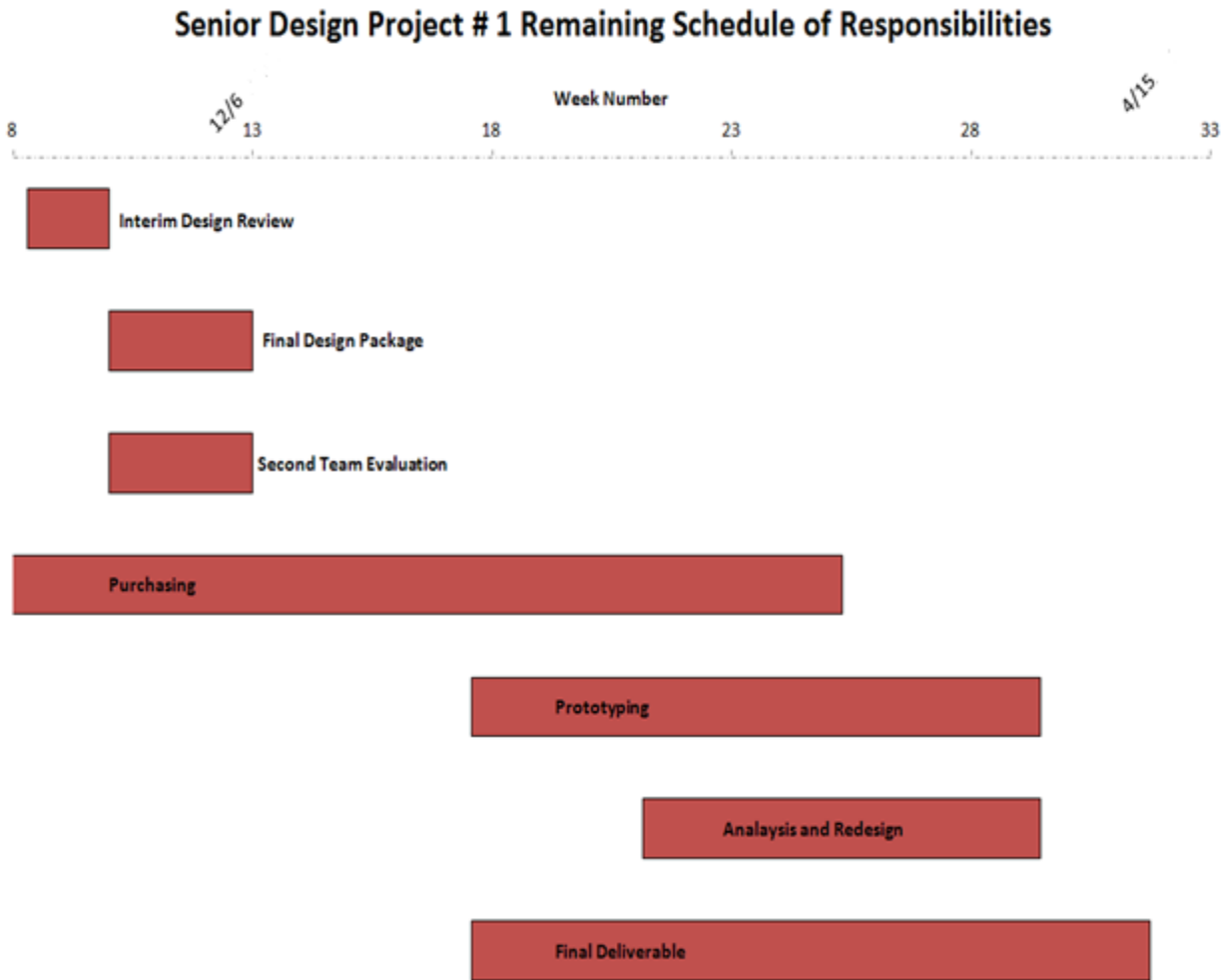


Figure 1 – Project Schedule

Concept Design –

In order to efficiently generate the design of the final SHPB prototype, the experiment was broken into subsections. Each section was studied, multiple concepts were produced, and

from those concepts the final choices were made. The physical subsections of the experiment were chosen to be the:

1. Base
2. Striker Bar Mechanism
3. Bars and Air Bushings
4. Strain Gages
5. Momentum Trap
6. Air Supply Manifold

In addition to the physical architecture of the design, a method of aligning the bushings to the proper tolerances as well as the data acquisition system to be used during testing needed to be determined. For each of these areas, the two most adequate concepts were also selected and chosen from.

Striker Bar Mechanism –

For the striker bar, the choice of designs came down to building a pendulum hammer or using an electric solenoid to propel a striker bar. The benefits of the pendulum hammer are that it is a cheap, mechanical way of producing a shockwave in the bars. The entire mechanism would cost less than \$50 in materials.

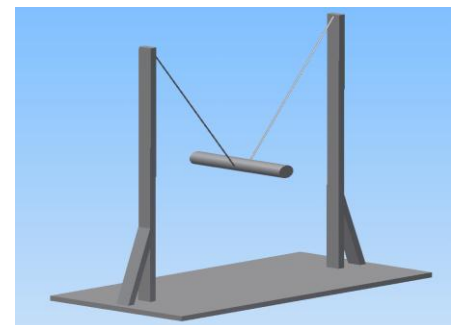


Figure 2 – Pendulum Hammer

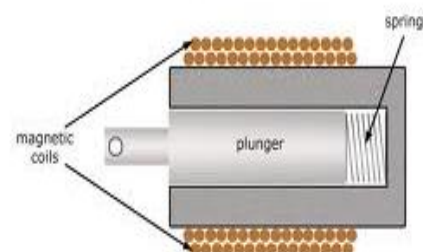


Figure 3 – Electric Solenoid

However, its design would require a large hammer mass to cause a strain high enough to deform a sample. Also, given that the hammer would be suspended by ropes or cables, assuring a proper impact between it and the incident bar could prove difficult. On the other hand, an electric solenoid should be able to consistently propel a striker bar at a known speed. By constraining the bar within a tube, its impact with the incident bar could be controlled. A solenoid capable of producing enough force to drive a 0.75 inch striker bar to the required speeds costs between \$60 and \$100. Since the cost is not significantly greater and the velocity of the striker bar can be more easily controlled, it was decided that the final design would implement a solenoid.

Table 1 - Striker bar mechanism decision matrix

	Weight	Pendulum Hammer	Electric Solenoid
Cost	0.2	4	3
Simplicity	0.2	5	3
Accuracy	0.3	3	5
Durability	0.2	4	5
Weight	0.1	4	4
<u>Weighted Score</u>	1.0	3.9	4.1

Incident and Transmitted Bars/ Air Bushings –

Since the size of the incident and transmission bars would directly determine the size of the air bushings, and vice versa, the bars and bushings were

considered in parallel. The choices of diameter of the bars and bushing were narrowed to 0.5 inch and 0.75 inch options

because of overall size, cost, and availability. The final choices of these components came after some analysis of the striker bar

mechanism. It was mathematically determined that by using a 0.75 inch bars, producing the amount of strain required to

deform a copper sample would be more easily achieved. This also should benefit the group during the Spring 2012 semester

when strain gages must be applied to the bars. It is believed that

the larger the diameter of the bars, the easier the application of the strain gages will be. As for

the costs of the bushings, New Way Air Bearings and Nelson Air Corp. were contacted as to the prices and specifications of their products. In both price and robustness, New Way Air Bearing's

products were seen to be superior. New Way bushings cost approximately \$50 less than those of Nelson Air while supporting 50% more radial load. Using McMaster-Carr, the price difference

between bars of 0.5 and 0.75 inches would not be an issue. Precision 1566 steel shafts cost \$20 and \$30 for 0.5 and 0.75 inch bars, respectively. As is shown by the decision matrices below, it

was decided to implement 0.75 inch air bushings and rods in the final design.



Figure 4 – Air Bushings



Figure 5 – Steel Rods

Table 2 - Incident and transmitted bar decision matrix

	Weight	0.5''	0.75''
Cost	0.1	4	3
Weight	0.2	4	4
Size	0.1	5	5
Durability	0.2	5	5
Portability	0.1	4	4
Accuracy	0.2	3	4
Data Quality	0.1	3	4
<u>Weighted Score</u>	1.0	4.0	4.2

Table 3 - Air bushing decision matrix

	Weight	New Way	Nelson Air
Cost	0.2	3	2
Weight	0.2	5	5
Size	0.1	5	5
Durability	0.2	5	4
Portability	0.1	5	5
Accuracy	0.2	5	4
<u>Weighted Score</u>	1.0	4.6	4

Base –

The choice for constructing the prototype’s base came down to using an I-beam or constructing a foundation using T-slotted framing. The I-beam would cost less than \$100, it would have high strength, its design would allow for simple alignment of the bushings, and it would be completely scalable. However, due to the size of the I-beam, its weight could cause the portability of the final design to be reduced. On the other hand, the T-slotted framing would require around \$120 worth of material to construct the base, would be lightweight, its geometry

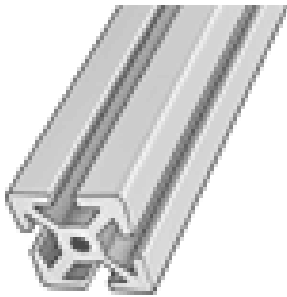


Figure 6 – T-Slotted Framing

would allow it to create a very rigid base, and its scalability is excellent. As can be seen in the decision matrix below, the T-slotted framing was chosen to be best for use in the design.

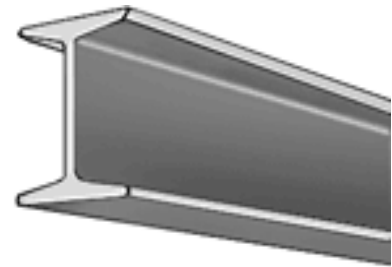


Figure 7 – I-Beam

Table 4 - Base decision matrix

	Weight	I – Beam	T-Slot
Cost	.3	3	5
Simplicity	.2	4	4
Weight	.2	2	4
Portability	.3	4	5
<u>Weighted Score</u>	1.0	3.3	4.6

Data Acquisition/ Air Supply -

The choices of data acquisition system and air supply manifold type were not as crucial at this stage of the project as the choice of the other sections. Early on it was decided that the air manifold would be composed of a 4 to 6 foot steel pipe which used flexible tubing to deliver air to the individual bushing blocks. The main air supply would come either from a compressor or a pressurized tank of air. The pipe would have a purge valve as well as shut off valves for each of the bushings. This would be done to ensure that if liquid or other contaminants were to make their way into the manifold, a method of isolating the bushings and flushing the system was available. The only choice to be made was to either set the manifold at an incline or to lay it horizontally. As the inclined version would simply complicate construction, the horizontal version was chosen. The choice of data acquisition came down to deciding between LabVIEW and MatLab. At the FSU Engineering College, it was found that LabVIEW was the more available of the two options and was therefore chosen as the system to be used in the testing portion of the project.

Strain Gauges –

When researching types of strain gauges to implement in the SHPB system, the two best options found were foil and semiconductor gauges.

The companies which produce the foil and semiconductor gauges in question are Vishay and

Micron-Instruments, respectively. Foil strain

gauges work due to the deformation of a strain

sensitive pattern. This pattern is etched out of a

metal foil and placed securely onto a backing. Once firmly applied to a piece of material,

deflection of that material is transferred to the foil pattern and a change in electrical resistance is

caused. Semiconducting gauges work by replacing the foil pattern with a doped semiconducting material which also responds to geometric changes with changes in electrical resistance. As for

pros and cons, foil gauges are durable, cost \$10 to \$20 each, and are a proven method of strain

detection. Their only downside may be their low gage factor. Vishay foil gauges have a factor of approximately 2. Gage factor is the measure of a gages response to a given amount of strain.

The higher the gage factor the greater the response to a given amount of strain. Semiconducting

gages exhibit higher gage factors than do foil gauges. Micron-Instruments list their gauges as

having factors in the 140 range. This would allow for them to be used in situations where the

amount of strain is so small as to not be detected using a foil gage. However, a drawback to is

that semiconductor gauges do not have the durability of foil gauges and are therefore are more

easily damaged during installation and operation. As for cost, Micron-Instrument's

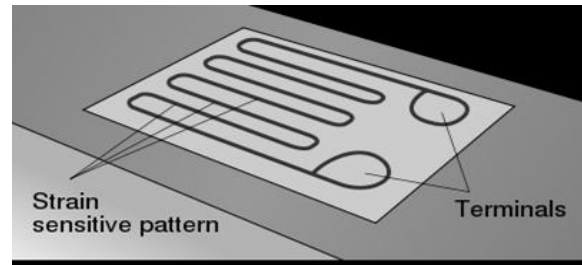


Figure 8 – Foil Strain Gage



Figure 9 – Semiconductor Strain Gage

semiconductor gages are also \$10to \$20 each if bought individually, but can cost between \$80 and \$160 for a matched set of 4 gages. In the decision matrix below, it is seen that the semiconducting gages were believed to be the better choice. However, Micron Instruments was contacted as to some of the specifications of their gauges and the intention of this project was discussed. For the purpose of this project, Micron-Instruments suggested the use of foil gages unless it was determined that the use of semiconducting gages was absolutely required. Also, upon contact with Vishay it was found that student rates as low as 10 gauges for \$20 were available. Given this turn of events, foil gages will be used in the final design.

Table 5 - Strain gauges decision matrix

	Weight	Foil	Semiconductor
Cost	0.2	3	2
Size	0.1	5	5
Data Quality	0.2	5	4
Durability	0.1	5	5
Ease of Use	0.2	5	4
<u>Weighted Score</u>	1.0	4.6	4

Momentum Trap -

In order to maintain the functionality of an SHPB experiment, a device must be constructed that will decelerate the incident and transmission bars after a test has been run. This function is the purpose of the momentum trap. For this design, the requirements set up for the trap are simply that it will have the ability to absorb the impact of the bars while having low cost. The two options which were chosen from were construction of a custom bumper or the use of a premade device. As for the benefits of both types, they are low cost, replaceable, and have the ability to absorb significant impacts. In the final decision, as seen in the decision matrix below, the choices were very close in all areas of concern. When the final decision was made, it was determined that a custom trap would be the best choice because it is the most easily scaled of the two choices.

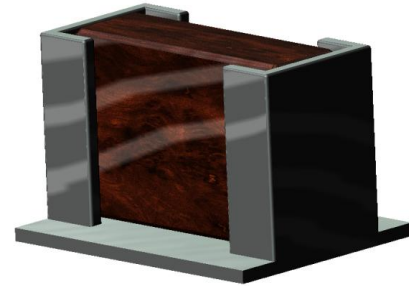


Figure 10 – Custom Momentum Trap



Figure 11 – Manufactured Bumper

Table 6 - Momentum trap decision matrix

	Weight	Custom	Prefabricated
Cost	0.2	4	4
Weight	0.1	4	3
Size	0.1	3	3
Simplicity	0.1	4	4
Durability	0.25	4	3
Scalability	0.15	4	3
Ease of Use	0.1	4	4
<u>Weighted Score</u>	1.0	3.9	3.4

Bushing Alignment -

As for the decision regarding bearing alignment, it was determined early on that some type of laser based alignment would be used to place the bushings in the correct

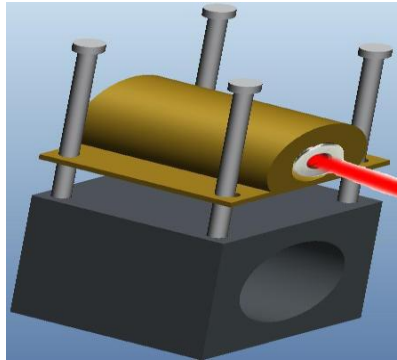


Figure 12 – Exterior Alignment

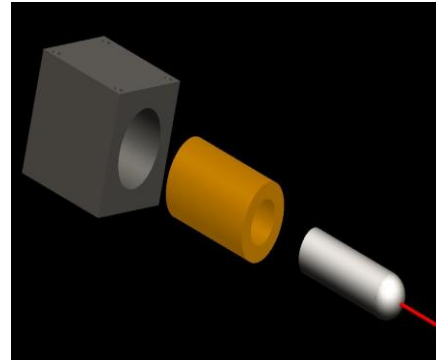


Figure 13 – Center Bore Alignment

relationship with each other. The two methods which were chosen from were very similar. The major difference is that with one the laser would be mounted on the top of the bearing blocks and with the other it would be mounted in the center of the block. These choices were labeled as

center-bore and exterior alignment. As can be seen below, the final choice of the group was to use the center bore alignment method. This was chosen because of the accuracy with which the laser could be mounted relative to the bushing block's center axis. The alignment of the blocks will be done with the laser being mounted within one block and a small target mounted within the next. When the laser illuminates the correct portion of the target insert, the two blocks will be aligned.

Table 7 - Bushing alignment decision matrix

	Weight	Center-Bore	Exterior
Cost	0.2	3	3
Simplicity	0.1	2	4
Scalability	0.2	4	3
Accuracy	0.4	5	4
Ease of Use	0.1	5	3
<u>Weighted Score</u>	1.0	4.1	3.5

Decision Matrix -

		Decision Matrix											
		Cost	Weight	Size	Simplicity	Durability	Portability	Scalability	Accuracy	Data Quality	Ease of Use	Score	
Base	Weight	0.3	0.2	N/a	0.2	N/a	0.2	N/a	0.3	N/a	N/a	N/a	
	I-beam	3	2		4			4				3.3	
	T-slot	5	4		4			5				4.6	
Bushing	Weight	0.2	0.2	0.1	N/a	0.2	0.2	0.1	N/a	0.2	N/a	N/a	
	New Way	3	5	5	5			5		5		4.6	
	Nelson	2	5	5	5			4		4		4	
Strain Gauges	Weight	0.2	N/a	0.1	N/a	0.2	N/a	0.2	N/a	N/a	0.3	0.2	
	Foil	4		4				5			3	4	
	Semiconductor	3		5				4			5	4	
Bar *	Weight	0.1	0.2	0.1	N/a	0.2	0.2	0.1	N/a	0.2	0.1	N/a	
	1/2 inch	4	4	4	5			4		3	3	4	
	3/4 inch	3	4	4	5			4		4	4	4.2	
Striker Bar	Weight	0.2	0.1	N/a	0.2	0.2	N/a	N/a	0.3	N/a	N/a	N/a	
	Solenoid	3	4		3			5		5		4.1	
	Pendulum	4	4		5			4		3		3.9	
Air Manifold	Weight	0.2	0.1	0.2	0.1	0.2	0.2	0.2	N/a	N/a	N/a	N/a	
	Horizontal	3	3	3	5			3				3.4	
	Declined	3	3	3	3			3				3.2	
Bearing Alignment	Weight	0.2	N/a	N/a	0.1	N/a	N/a	0.2	0.2	0.4	N/a	0.1	
	Insert	3			2			4		5		5	
	Mounted	3			4			3		4		3	
Momentum Trap	Weight	0.2	0.1	0.1	0.1	0.1	0.25	N/a	0.15	N/a	N/a	0.1	
	Custom	4	4	3	4			4		4		4	
	Prefabricated	4	3	3	4			3		3		4	
												3.4	

Final Design –

By combining the final design choices, the overall design shown below was formed. It should be noted here that the air manifold system is not represented in this drawing in order to more clearly show the other sections of the design. When mounted, the manifold would simply run parallel to the bars along the edge of the design.

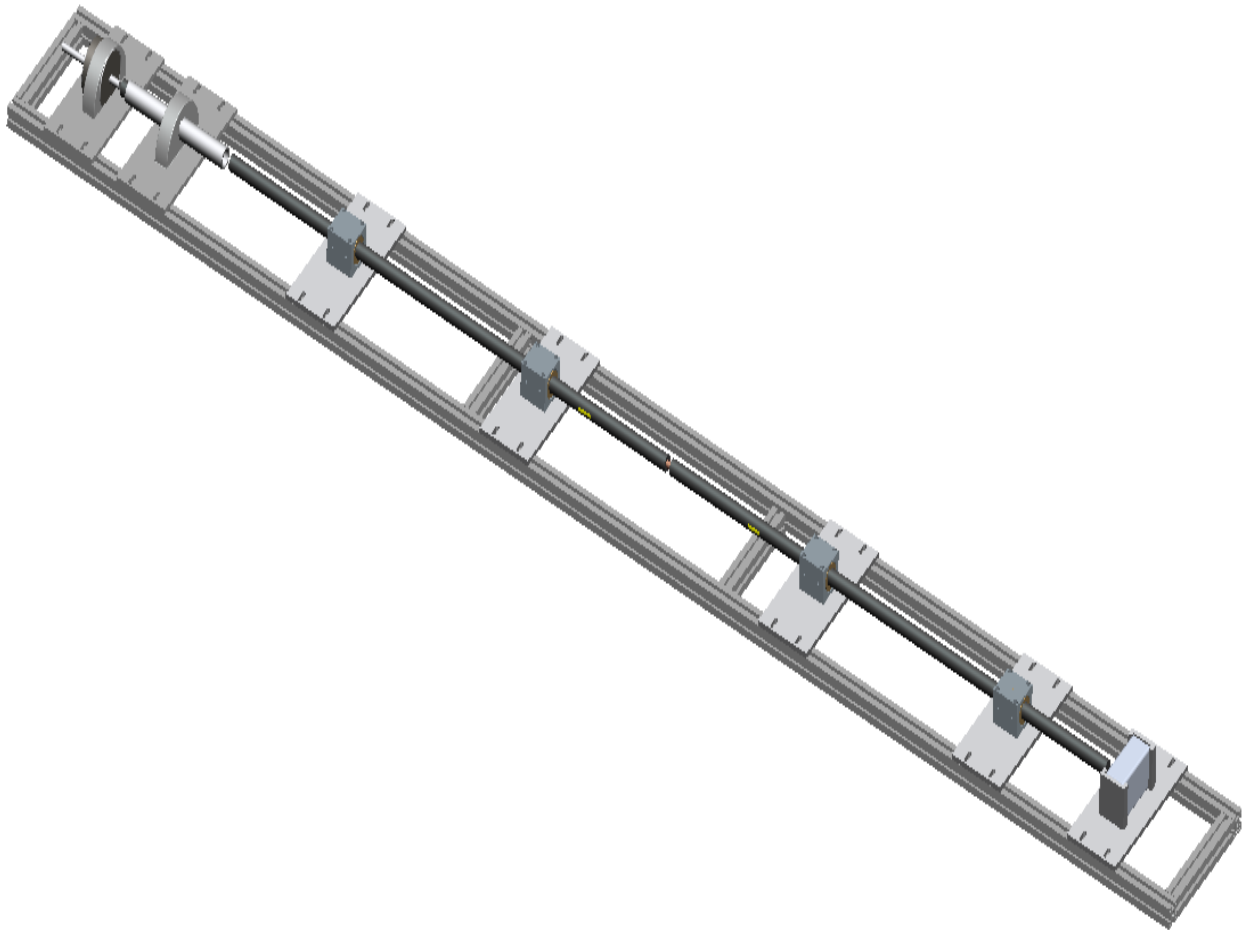


Figure 14 – Final Design

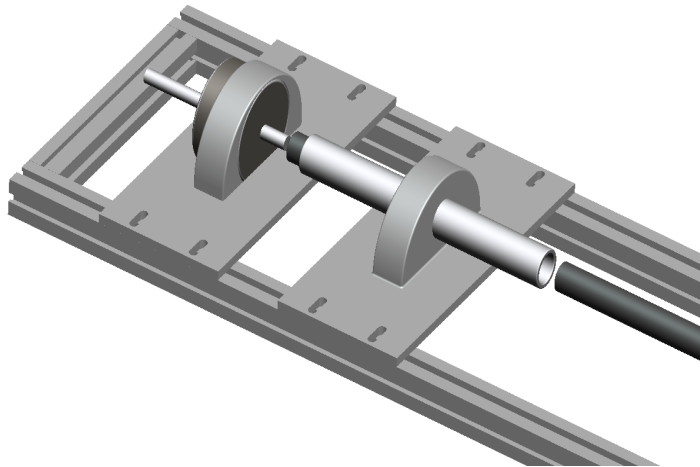


Figure 15 – Striker Mechanism

The picture to the left shows the striker mechanism of the final design.

Consisting of a solenoid mounted in an aluminum cross-plate, a striker bar, as well as a guide tube to ensure correct alignment between the striker and incident bars during impact, this mechanism should provide consistent

striker bar velocities and repeatable test conditions. Next is a close up image of a single air bushing with the bushing block, bushing, and steel bar installed. There will be a total of 4 air bushings used in this design. Below is a picture of where the incident and transmitter bars meet and hold a small material sample. Also, the placement of the strain gages is also shown in this picture by the small yellow strips placed on the bars.

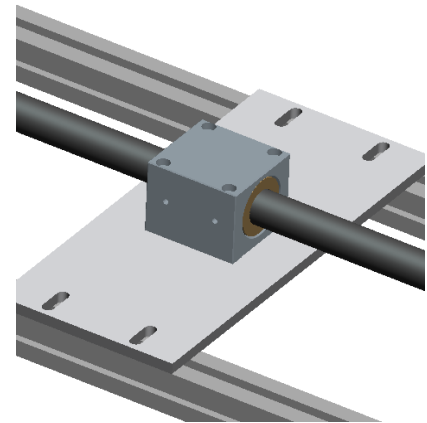


Figure 16 – Air Bushing

The custom momentum trap design is also shown below.

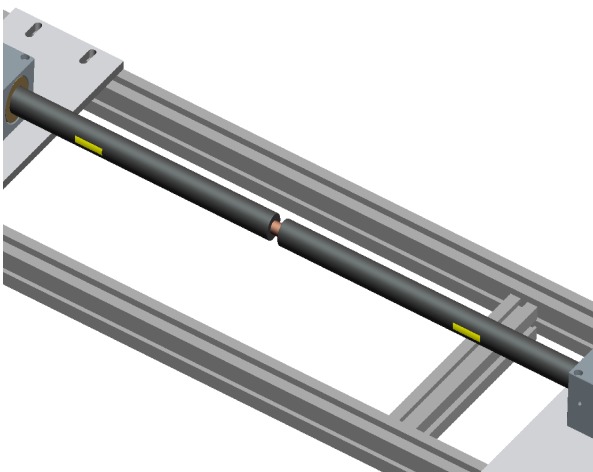


Figure 17 – Bars, Sample, and Strain Gages

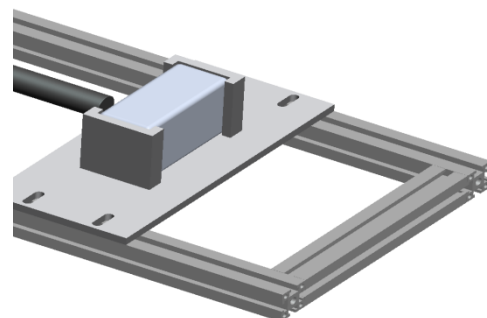


Figure 18 – Custom Momentum Trap

Cost Analysis -

Senior Design Group #1: Preliminary Cost Analysis

Budget	\$2,500.00
Total Cost	\$1,614.80
Remaining	\$885.20

Item	Quantity	Unit Cost	Total Cost
Air Bushings 0.75 inch	4	\$331.00	\$1,060.00
Solenoid	1	\$69.94	\$69.94
T-slot Framing 1 1/2 inch (96 inch length)	2	\$48.15	\$96.30
T-slot Framing 1 1/2 inch (4 foot length for 6 inch braces)	1	\$25.15	\$25.15
Incident & Transmission Bar: 1566 Steel Bar 0.75 inch (36inch length)	2	\$29.42	\$58.84
Air Manifold (72 inches)	1	\$16.34	\$16.34
T-slot Framing 1 1/2 inch (24 inch length) For stability	1	\$13.98	\$13.98
Striker Bar: 1566 Steel Bar 0.75 inch (12inch length)	1	\$10.25	\$10.25
DAQ			\$0.00
Momentum Trap			\$0.00
Air supply			\$0.00

Analysis -

For the design of any engineered metallic item in which the behavior of the material under static or dynamic loading is significant, a statistically relevant reproducible trend. To begin, the force applied has to be standardized through a force/material density. Assuming the force is only in one direction, the stress through a unit of area is given as:

$$\sigma = F/A \quad \text{Eqn. 1}$$

where σ = stress F = force and A = instantaneous area

In cases of loading where the change in the length of the material under loading is needed the change in length is given as a percentage of the initial length as:

$$\varepsilon = (L_i - L_o) / L_o \quad \text{Eqn. 2}$$

where ε = strain L_i = instantaneous length L_o = initial length

The SHPB experiment loads three piece of metal in two different ways. The incident and transmitter bar are loaded elastically. See the SHPB section for more detail. That is the loading occurs and the material stretches or compresses and then after the loading ceases, the material returns to its original length, with no permanent crystal deformation, or “slip” along the microscopic planes of atoms. The point at which the material begins to permanently deform is called the yield point. Inside of the elastic region of deformation the relationship between stress and strain is linear. The ratio of this relationship is specific to each material. This ratio is called the Young’s Modulus E given as:

$$\sigma = E * \varepsilon \quad \text{Eqn. 3}$$

This elastic behavior is necessary for the SHPB experiment to be quantified. The measurement taken from each of the elastically loaded bars is the strain ε . The strain is measured

by a strain gauge. A strain gauge uses the physical changes caused by strain to be measured as a change in resistivity in a resistor set. The strain gauge has a ratio of the change in resistance divided by the strain passing through the material being tested. This ratio is called the gauge factor and is given as:

$$GF = [(R_i - R_g) / R_g] / \epsilon \quad \text{Eqn. 4}$$

Where GF = gauge factor R_i = instantaneous resistance R_g = initial resistance and ϵ = strain

So therefore if the desired strain at a given time is desired, one can rearrange the equation to be:

$$\epsilon = [(R_i - R_g) / R_g] / GF \quad \text{Eqn. 5}$$

Where GF = gauge factor R_i = instantaneous resistance R_g = initial resistance and ϵ = strain

This allows the strain to be the output of the given input of R_i from the resistor set.

The Resistor set is based on a Wheatstone circuit. This circuit allows for precise measurements of the resistance inside of the stress gauge resistor. The Wheatstone circuit contains four resistors, three of which have resistances of known value, and one is the stress gauge resistor. The relationship between them is as follows

$$R_g = (R_2 / R_1) * R_3 \quad \text{Eqn. 6}$$

Where R_g = stress gauge resistance and R_1 , R_2 and R_3 are known resistances.

The voltage difference between the two interior junctions is the measured output. The governing equation is given as follows:

$$V_g = [(R_g / \{ R_3 + R_g \}) - (R_2 / \{ R_1 + R_2 \})] * V_a \quad \text{Eqn. 7}$$

Where V_g = measured voltage R_g = stress gauge resistance R_1 , R_2 , and R_3 = known Resistances and V_a = applied voltage

This instantaneous strain is recorded with respect to time. This measurement is taken in two places: The incident bar and the Transmitter bar. The gauges give three strain wave measurements: 1) an Incident wave through the incident bar ϵ_I 2) A reflected wave through the incident bar ϵ_R and 3) An incident wave through the transmitter bar ϵ_T . Given that the initial length of the specimen and the speed of sound through the specimen material are known, then both the average engineering strain rate as well as the total strain can be calculated using the following equations:

$$d\epsilon_{avg}/dt = (C_b / L_s) * (\epsilon_I - \epsilon_R - \epsilon_T) \quad \text{Eqn. 8}$$

Where $d\epsilon_{avg}/dt$ = average engineering strain rate and L_s = initial length of the specimen.

$$\epsilon_s = (C_b / L_s) * \int_0^t [(\epsilon_I - \epsilon_R - \epsilon_T) * dt] \quad \text{Eqn. 9}$$

Where ϵ_s = strain in the specimen

As discussed before the strain must have a corresponding stress to allow for computation of the Young's Modulus. The stress at the connection between the incident bar and the specimen is given as a ratio of the area of the two bars (as energy is conserved, the force that is transmitted through the large area of the incident bar must be transmitted into the small area of the specimen) the Young's modulus of the Incident bar and the Incident and Reflected waves as:

$$\sigma_I = (A_B / A_s) * E_B * (\epsilon_I + \epsilon_R) \quad \text{Eqn. 10}$$

The stress at the connection between the specimen and the transmitter bar is similar to before, but only the transmitted wave is taken into account as:

$$\sigma_2 = (A_B / A_s) * E_T \quad \text{Eqn. 11}$$

From this the average stress can be taken:

$$\sigma_{avg} = 0.5 * (\sigma_1 + \sigma_2) \quad \text{Eqn. 12}$$

The elastic strain energy in the incident bar due to the incident wave is given as :

$$E_I = 0.5 * A_B * C_B * E_B * T * \epsilon_I^2 \quad \text{Eqn. 13}$$

Where E_I = strain energy due to the incident wave A_B = cross sectional area of the bar
 C_b = Speed of sound in the bar T = amount of time the square loading wave was applied
 through the gauge.

The elastic strain energy is the same for the reflection and transmitted wave:

$$E_I = 0.5 * A_B * C_B * E_B * T * \epsilon_R^2 \quad \text{Eqn. 14}$$

$$E_I = 0.5 * A_B * C_B * E_B * T * \epsilon_T^2 \quad \text{Eqn. 15}$$

The strain energy used in the deformation of the specimen is given as

$$\delta S_E = E_I - E_R - E_T \quad \text{Eqn. 16}$$

The Kinetic energy is the energy of motion. The kinetic energy being transmitted by the waves are given as:

$$K_I = 0.5 * \rho_B * A_B * C_B^3 * T * \epsilon_I^2 \quad \text{Eqn. 17}$$

$$K_R = 0.5 * \rho_B * A_B * C_B^3 * T * \epsilon_R^2 \quad \text{Eqn. 18}$$

$$K_T = 0.5 * \rho_B * A_B * C_B^3 * T * \epsilon_T^2 \quad \text{Eqn. 19}$$

The strain energy used in the deformation of the specimen is given as:

$$\delta K_E = E_I - E_R - E_T \quad \text{Eqn. 20}$$

The total deformation energy in the specimen is given as:

$$E_s = 2 * \delta K_E = 2 * \delta S_E \quad \text{Eqn. 21}$$

Strain Gauges:

The strain gauges used in the SHPB experiment are electrical resistance gauges. They use the physical distortion in the width of the electrical conductors. The thinner the conductor becomes the more resistance it creates. The thicker the conductor becomes, the less resistance it creates. The placement of the strain gauge is such that as the material being tested is put into tension, the lengths of the gauge are being stretched and as such the resistance increases. If the material is put into compression, then the lengths of the gauge are being shortened and as such the resistance decreases.

The strain gauge has a ratio of the change in resistance divided by the strain passing through the material being tested. This ratio is called the gauge factor and is given as:

$$GF = [(R_i - R_g) / R_g] / \epsilon \quad \text{Eqn. 22}$$

Where GF = gauge factor R_i = instantaneous resistance R_g = initial resistance and ϵ = strain

So therefore if the desired strain at a given time is desired, one can rearrange the equation to be:

$$\epsilon = [(R_i - R_g) / R_g] / GF \quad \text{Eqn. 23}$$

Where GF = gauge factor R_i = instantaneous resistance R_g = initial resistance and ϵ = strain

This allows the strain to be the output of the given input of R_i from the resistor set.

The Resistor set is based on a Wheatstone circuit. This circuit allows for precise measurements of the resistance inside of the stress gauge resistor. The Wheatstone circuit

contains four resistors, three of which have resistances of known value, and one is the stress gauge resistor. The relationship between them is as follows

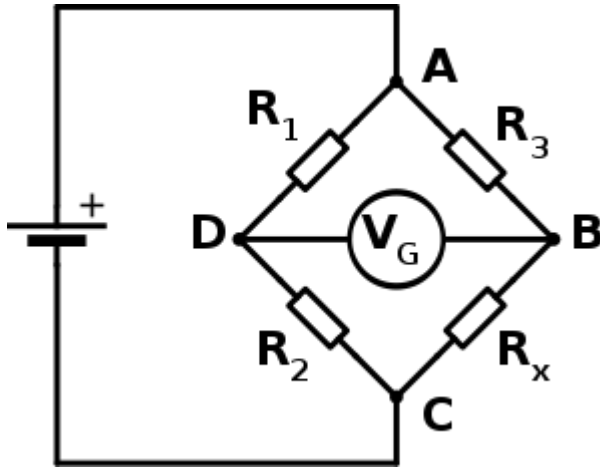


Figure 19 – Wheatstone Bridge Circuit

$$R_x = (R_2 / R_1) * R_3 \quad \text{Eqn. 24}$$

Where R_x = stress gauge resistance and R_1 , R_2 and R_3 are known resistances.

The voltage difference between the two interior junctions is the measured output. The governing equation is given as follows:

$$V_g = [(R_g / \{R_3 + R_x\}) - (R_2 / \{ R_1 - R_2\})] * V_a \quad \text{Eqn. 25}$$

Where V_g = measured voltage R_x = stress gauge resistance R_1 , R_2 , and R_3 = known Resistances and V_a = applied voltage

Striker Velocity Analysis/Solenoid optimization –

It is desired to have the velocity required of the striker bar to plastically deform the copper specimen to choose define the solenoid and other modeling factors. The following pages show the required process to choose the optimal Solenoid.

The velocity of the striker bar is needed the only requirement is that the specimen plastically deform while the incident and transmitter bars are only loaded elastically.

The following equations show the process

$$\sigma_{yc} := 172 \text{MPa} \quad \text{Eqn. 26} \quad \text{Compressive Yield stress of copper}$$

$$\text{Area}_c := \pi \cdot \left(\frac{.75}{4} \text{in} \right)^2 = 0.11 \text{in}^2 \quad \text{Eqn. 27} \quad \text{Area of the copper}$$

$$F_{yy} := \sigma_{yc} \cdot \text{Area}_c = 12.256 \text{kN} \quad \text{Eqn. 28} \quad \text{Force Required to reach Yield}$$

Next the mass of the steel bar is computed

$$\rho := 7.85 \frac{\text{gm}}{\text{cm}^3} = 7.85 \times 10^3 \frac{\text{kg}}{\text{m}^3} \quad \text{Eqn. 29} \quad \text{Density of steel}$$

$$v := \pi \cdot \left(\frac{0.75}{2} \right)^2 \text{in}^2 \cdot 6 \text{in} = 2.651 \text{in}^3 \quad \text{Eqn. 30} \quad \text{Volume of the 3/4 inch diameter, 6 inch striker bar}$$

$$\text{mass} := v \cdot \rho = 0.341 \text{kg} \quad \text{Eqn. 31} \quad \text{Mass of the striker bar}$$

Next the amount of time the striker bar will impact the incident bar

$$c := 6100 \frac{\text{m}}{\text{s}} \quad \text{Eqn. 32} \quad \text{Speed of wave propagation in steel}$$

$$L_s := 6 \text{in} \quad \text{Eqn. 33} \quad \text{Length of Striker bar}$$

$$t := 2 \cdot \frac{L_s}{c} = 4.997 \times 10^{-5} \text{s} \quad \text{Eqn. 34} \quad \text{Pressure wave propagating down the striker bar and returning} = 2 \times \text{length/speed}$$

$$t = 49.967 \mu\text{s} \quad \text{Eqn. 35} \quad \text{Duration of impact}$$

Finally the minimum velocity of the striker bar needed to plastically deform the specimen

It is also desired to choose a solenoid that will give this striker bar velocity at a minimum as well as not deform the steel bars. The Minimum velocity of striker bar needed to plastically deform the copper specimen

$$V := \frac{F}{\text{mass}} \cdot t = 1.796 \frac{\text{m}}{\text{s}} \quad V = 4.017 \frac{\text{m}}{\text{hr}}$$

Eqn. 36

compressive yield strength of the steel is 1220 MPa.

Therefore the fatigue strength at an infinite number of cycles is approximately 600 Mpa.

$$\sigma_{y\text{infinite}} = \frac{\sigma_y}{2} \quad \text{Eqn. 37}$$

$$\text{Acc} := \frac{3360z\text{f}}{\text{mass}} = 273.95 \frac{\text{m}}{\text{s}^2} \quad \text{Eqn. 38}$$

Acceleration available from a

chosen solenoid

$$L_{\text{sol}} := 1\text{in} \quad \text{Eqn. 39}$$

Length of piston with given force

$$D = D_0 + V_0 \cdot t + .5A_{\text{cc}} \cdot t^2 \quad \text{Eqn. 40} \quad \text{Generic dynamic position equation}$$

$$\text{time}_{\text{sol}} := \left(\frac{L_{\text{sol}}}{0.5 \text{Acc}} \right)^{.5} = 0.014\text{s} \quad \text{Eqn. 41} \quad \text{Derived time, from previous equation}$$

$$V_{\text{stkr}} := \text{Acc} \cdot \text{time}_{\text{sol}} = 8.345 \frac{\text{m}}{\text{hr}} \quad \text{Eqn. 42} \quad \text{Calculated velocity from given solenoid}$$

$$\text{Force}_{\text{striker.sol}} := \frac{V_{\text{stkr}} \cdot \text{mass}}{t} = 25.45\text{N} \quad \text{Eqn. 43}$$

Optimization and Analysis of the Solenoid

Using the finite element analysis program Comsol, the maximum applied stress for the steel (600 MPa) was achieved using approximately 60 kN, or a striker velocity of approximately 20 mi/hr. This then equates to a maximum ounce force (ozf) from the solenoid (with a 1 inch stroke) of over 2000. The most powerful available solenoid is 996 ozf. The minimum acceptable solenoid strength gives approximately 80 ozf. It is desired to have a factor of safety of 2 for the velocity of the striker bar. This gives a minimum desired solenoid strength of 310 ozf. It is also desired to have a maximum cost of the solenoid to be \$100. The following chart shows the graphical representation of the optimization of the choice in solenoid.

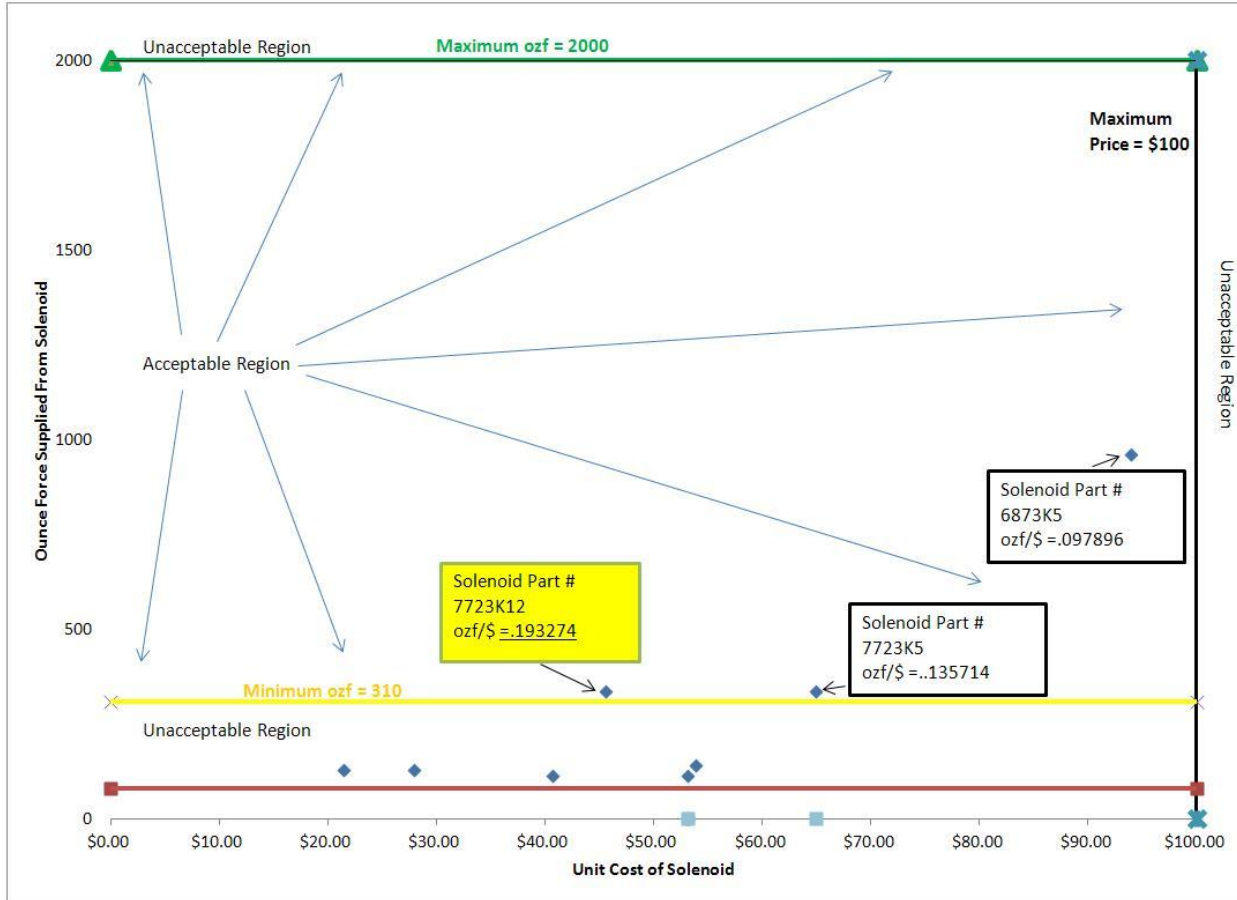


Figure 20 - Optimization graph

The optimization graph shows three borders for the acceptable region of the choice of solenoid: the maximum price (in black on the right side of graph) the minimum power (in yellow) and the maximum power (in green). The solenoid was then chosen as the one of the three in the acceptable region with the highest proportion of power per dollar. As the graph shows, the optimal solenoid is the 7723K12, which gives a total power output of 336 ozf with a cost of \$64.94 giving a ratio of 0.193274 ozf/\$.

Finite Element Analysis (FEM) –

Comsol Intro-

It has been requested that a stress analysis be performed around the specimen to check for maximum stresses as well as to show proof of concept of the shock wave passing through the system.

In order to properly use the FEA program Comsol, one must first develop the governing equations. The partial differential equations that govern this process are developed by axial motion along a bar:

$$\rho \cdot A \cdot \frac{d^2 T}{dt^2} - \frac{d}{dx} \left[E \cdot A \cdot \left(\frac{d u}{dx} \right) \right] - f(x, t) = 0$$

Eqn. 44

In order to eliminate the second order PDE, and create a simpler model for the computer to analyze, a weak form is developed. First one must multiply the equation by a weight factor w and integrate with respect to time and position:

$$\int \left[w \cdot \rho \cdot A \cdot \frac{d^2 T}{dt^2} - w \cdot \frac{d}{dx} \left[E \cdot A \cdot \left(\frac{d u}{dx} \right) \right] - w f(x, t) \right] dx = 0$$

Eqn. 45

Then one must use integration by parts or the product rule to remove the second order PDE:

$$\int \left[-(\rho \cdot A) \cdot \left(\frac{d w}{dt} \right) \cdot \left(\frac{d T}{dt} \right) - w f(x, t) \right] dx + w \cdot A \cdot \rho \cdot \left(\frac{d T}{dt} \right) = 0$$

Eqn. 46

This form of the equation can be integrated into the Comsol program easily, using discretization matrices to give exacting solutions, or using coefficients directly into the PDE function after defining a geometry. The matrix method would include the following matrices:

$$[K]\{u\} + [C]\{\dot{u}\} + [M]\{\ddot{u}\} = \{F\}$$

$$K_{ij} = \int_{x_a}^{x_b} \left[a(x) \cdot \left(\frac{d}{dx} \psi_i \right) \cdot \left(\frac{d}{dx} \psi_j \right) + c(x) \psi_i \cdot \psi_j \right] dx$$

$$M_{ij} = \int_{x_a}^{x_b} c_o(x) \cdot \psi_i \cdot \psi_j dx$$

Eqn. 47 Eqn. 48 Eqn. 49

where ψ_i and ψ_j are the weight and position functions respectively.

Comsol analysis –

After creating the correct geometry in the Comsol program and programming the coefficients of the materials in, then running a 5 microsecond force flux through the outer boundary of the incident bar the following was observed around the specimen:

a) The proof of concept that a strain wave traveling through a line 6.5 inches from the boundary between the incident bar and the specimen would roughly follow a square wave:

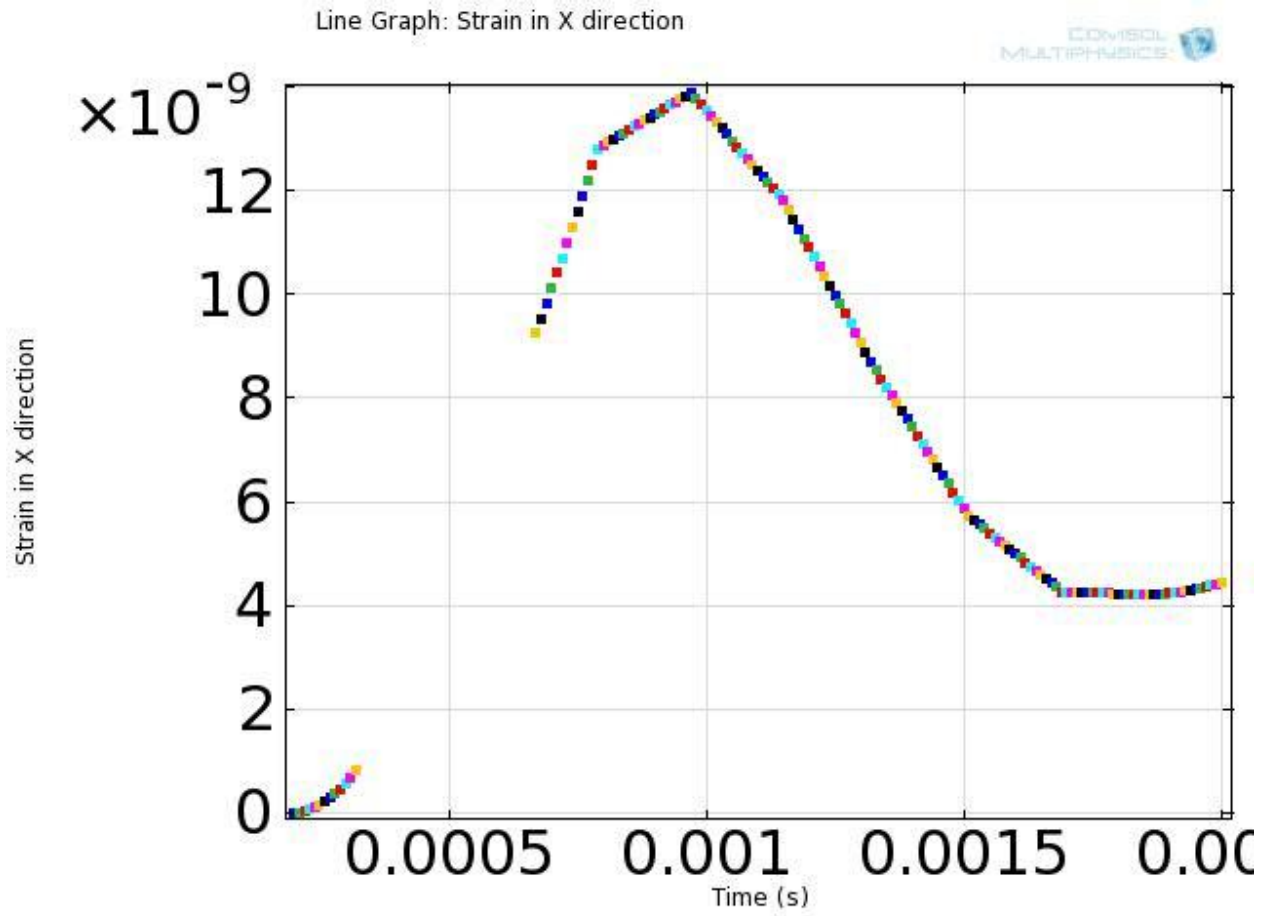


Figure 21 - Strain plot

b) Proof that at the peak force readings the stress in the copper would exceed the compressive yield stress limit ($400 \text{ MPa} > 172 \text{ MPa}$), while simultaneously showing that the stress felt in the steel would be less than the fatigue limit for the compressive yield of steel ($270 \text{ MPa} < 600 \text{ MPa}$)

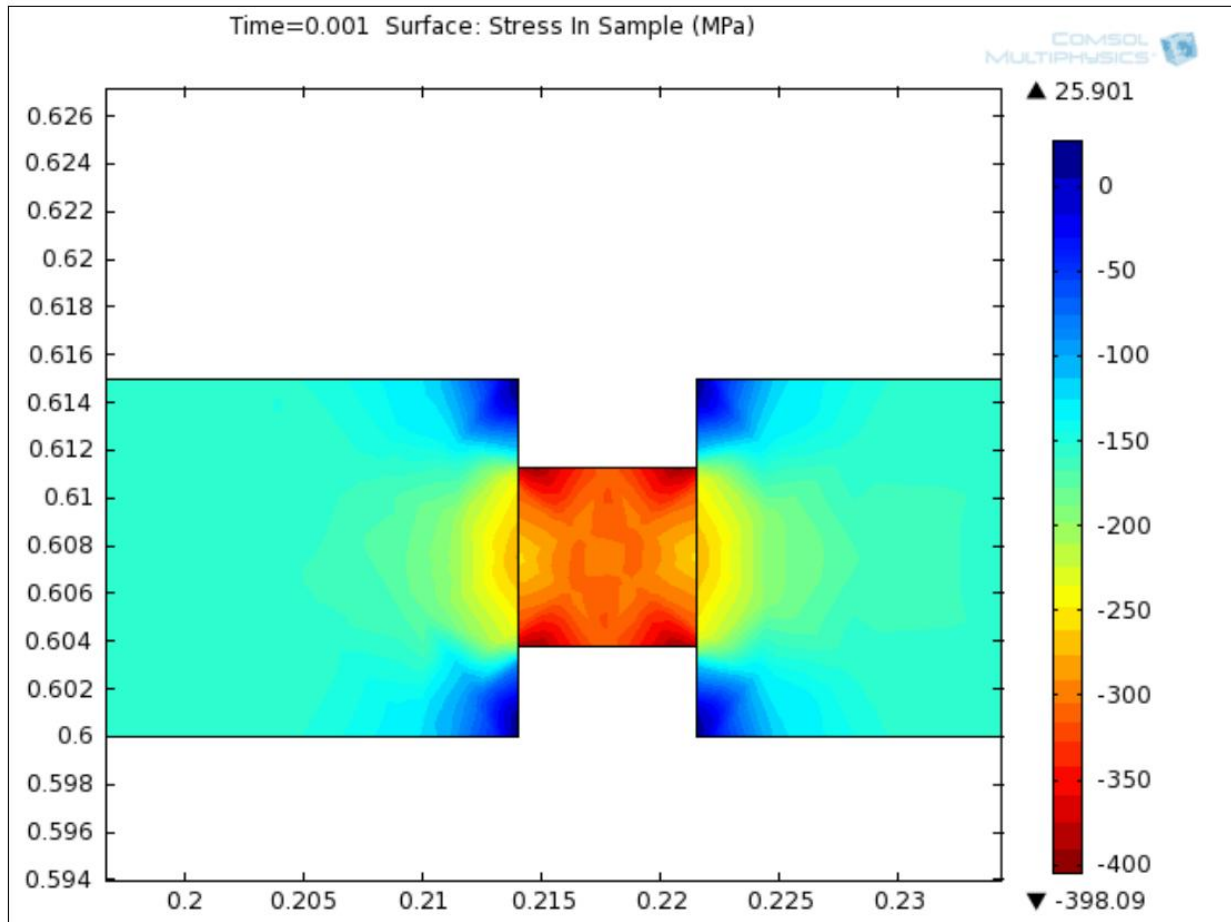


Figure 22 - Surface stress analysis

Environment and Safety –

The building and operation of the Split Hopkinson Pressure Bar apparatus will cause no harm to the environment. There are no harmful fluids or release of radiation that could leak out into the surroundings. Therefore, there are no health hazards due to inhalation or skin contact of a toxic substance. This project can be said to be environmental friendly.

In the process of building the SHPB device, several safety measures need to be accounted for. It is important to be careful when carrying and assembling the components of the apparatus. The heavier parts such as the bars must be carried with two hands. It would be best for at least two people to carry the T-slot and to assemble it for the support of the system. These safety steps for carrying each component are instilled to lessen the chances of a particular part falling on the foot of the persons carrying it or another person nearby. Also, there must certainly be no horse playing with the components. For example swinging the bars can result in serious injury.

Another set of safety measures are required when the SHPB device is in operation. No hands should be on any part of the SHPB model after the striker solenoid is released. Due to the high velocity of 6.31 m/s, the striker bar could potential snap off a finger. Also, the forces generated to the bars could damage someone's finger. A certain amount of distance should be kept from the apparatus when in operation to ensure that safety is maintained.

Conclusion –

One of the purposes of the project for this semester was to upgrade the air bearings for the 0.625" Split Hopkinson Pressure Bar at the Eglin Air Force Research Laboratory. After researching two companies, New Way Air Bearings and Nelson Air, New Way was selected for

the ordering of the air bushings. It was discovered that New Way had cheaper bushings and they were more efficient.

Another purpose for the project this semester was to make the preparations for the smaller SHPB model to be built here at the FAMU/FSU College of Engineering. It was chosen to build an 8' model SHPB as a replica of the much larger one at Eglin. The goal of the smaller model is not to produce data of high accuracy but to see if some data can be generated through a data acquisition system (Labview). It is expected that the proper mechanics of the replica are matched with that of the larger SHPB at Eglin. The new things that are to be developed are the laser alignment mechanism and the 6" solenoid used for the striker bar to provide constant velocity to the system. Also, a base using a T-slot will be implemented for the support of the entire device. The bar size for the 3' incident and transmitted bars will be increased to 0.75" because it will be better to work with a larger diameter bar, and a larger difference in area between the bars and the specimen produces a better square wave signal. Also, it will be quicker to receive the air bushings because they are available in New Way's inventory and do not have to be custom made unlike the 0.625" air bushings. Clean air will be supplied to the bushings from the air manifold pipe through polyurethane tubing. The wooden momentum trap will absorb the energy of the entire device. When the Split Hopkinson Pressure Bar model is built next spring semester it is expected that it will be a good representation of the SHPB at Eglin.

References –

- NewWayAirBearings. "Porous Media Technology." *New Way Air Bearings*. Web. 09 Oct. 2011. <<http://www.newwayairbearings.com/Porous-Media-Technology>>.
- New Way Air Bearings, Inc. *Porous Media Air Bearing Solutions*. Aston: New Way Air Bearings, 2010. *New Way Air Bearings*. 2010. Web. 9 Oct. 2011. <http://www.newwayairbearings.com/adx/asp/adxGetMedia.aspx?DocID=19,16,12,3,1,Documents&MediaID=5010&Filename=new_way_line_brochure_air_bushings_combined_nwab-10-m-037-v05-2010-05-17-2500_page.pdf>.
- "SCFM versus ACFM and ICFM." *Engineering ToolBox*. Web. 09 Oct. 2011. <http://www.engineeringtoolbox.com/scfm-acfm-icfm-d_1012.html>.
- "Care and Air." *New Way Air Bearings*. Web. 09 Oct. 2011. <<http://www.newwayairbearings.com/Care-And-Air>>.
- Omega Engineering. "The Strain Gauge". *Omega Engineering*. 09 Oct. 2011. <<http://www.omega.com/literature/transactions/volume3/strain.html>>
- "Strain Gauge." Wikipedia, the Free Encyclopedia. Web. 26 Oct. 2011. <http://en.wikipedia.org/wiki/Strain_gauge>.
- Chen, Weinong W., and Bo Song. Split Hopkinson (Kolsky) Bar: Design, Testing and Applications. New York: Springer Verlag, 2010. Print.
- "Electrical Strain Gauges." This Is Bits.me.berkeley.edu. Web. 26 Oct. 2011. <http://bits.me.berkeley.edu/beam/sg_2a.html>.
- "Capacitance Measurement Systems: Non-contact Measurement Sensors, Solutions and Systems –
- MTI Instruments." Non-contact Measurement Sensors, Solutions and Systems, Laser, Fiber Optic & Capacitance Sensors - MTI Instruments. Web. 26 Oct. 2011. <<http://www.mtiinstruments.com/products/capacitancemeasurement.aspx>>.
- "Micron Instruments - Bar Gage." Micron Instruments - Corporate Home Page. Web. 26 Oct. 2011. <<http://www.microninstruments.com/store/bargage.aspx>>.
- Green, Thomas M. "MatLab Intro. Thomas M. Green." Web. 26 Oct. 2011. <<http://www.contracosta.edu/legacycontent/math/Lmatlab.htm>>.
- "NI LabVIEW - Improving the Productivity of Engineers and Scientists." National Instruments: Test, Measurement, and Embedded Systems. Web. 26 Oct. 2011. <<http://www.ni.com/labview/>>.
- "Air Bushings." New Way Air Bearings. 21 October 2011.

- <http://www.newwayairbearings.com/Default.aspx?DN=e05778a6-99a1-c9c95e516d41>.
- "Mounting Components." New Way Air Bearings. 21 October 2011. <<http://www.newwayairbearings.com/Mounting-Components/>>
 - "Metals" Online Metals. 22 October 2011. <<http://www.onlinemetals.com/>>
 - McMaster-Carr. McMaster-Carr. Web. 26 Oct. 2011. <<http://www.mcmaster.com/>>.
 - Faztek. Faztek, LLC. Web. 26 Oct. 2011. <<http://faztek.rtrk.com/?scid=1322663>>.
 - "ThinkGeek :: Blue Violet Laser Pointer." ThinkGeek :: Stuff for Smart Masses. Web. 26 Oct. 2011. <<http://www.thinkgeek.com/gadgets/lights/b847/>>.
 - NorthernTool. "Klein Tools Rare Earth Magnet Torpedo Level —9in., Model# 931-9RE | Torpedo Levels |
 - Northern Tool Equipment." Portable Generators, Pressure Washers, Power Tools, Welders | Northern Tool Equipment. Web. 26 Oct. 2011. <http://www.northerntool.com/shop/tools/product_200357997_200357997>.
 - "Red Laser Pointer Torch Key Chain Fantastic as a Star-pointer - Easily Visible at Night Time." Laptop Battery Online, Battery Charger And Electronic Accessories Factory. Web. 26 Oct. 2011. <<http://www.my-batteries.net/laserpointer/red-laser-pointer-with-key-chain.htm>>.
 - "Light Gas Gun." Wikipedia, the Free Encyclopedia. Web. 27 Oct. 2011. <http://en.wikipedia.org/wiki/Light_gas_gun>.

Appendix A –

Complete Cost analysis

Senior Design Group #1:

Preliminary Cost Analysis

Budget \$2,500.00

Total Cost \$1,614.80

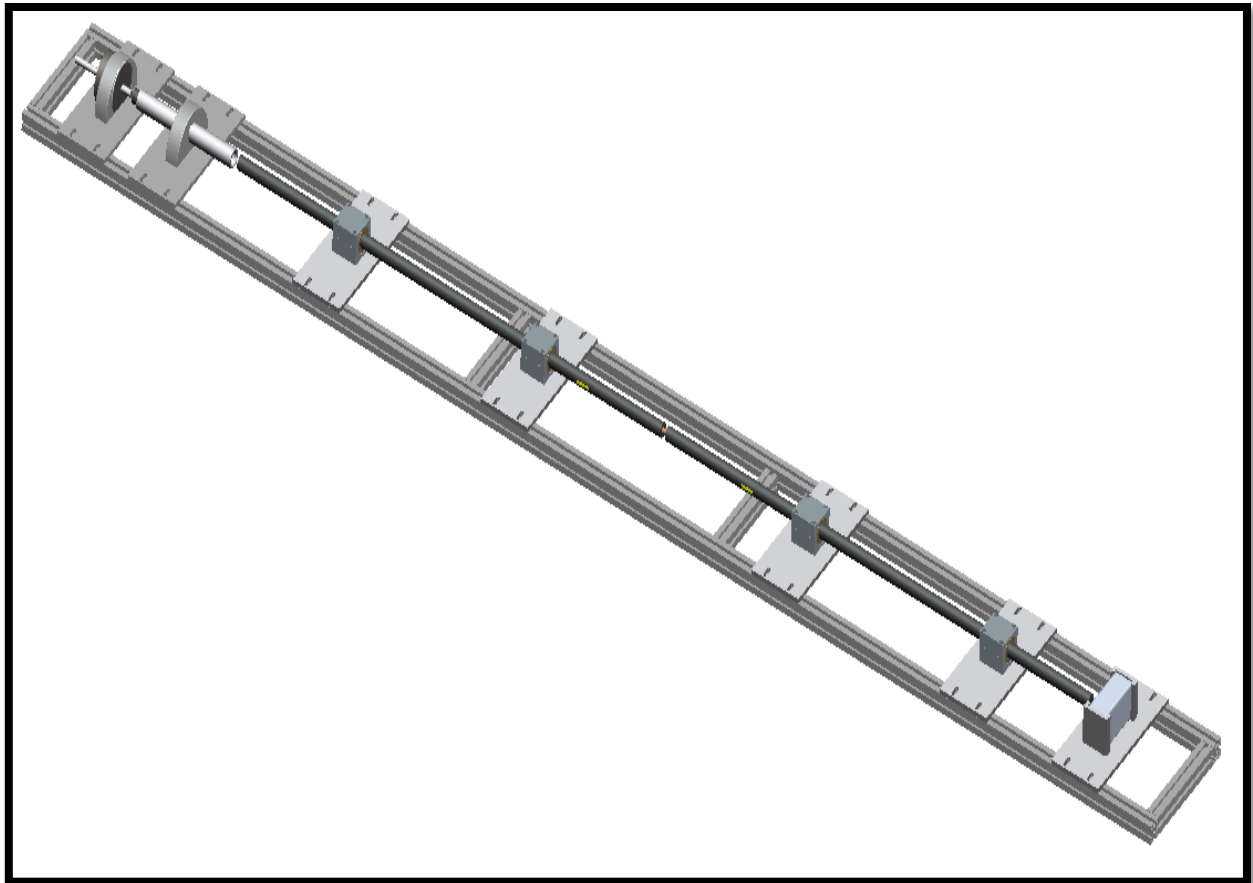
Remaining \$885.20

Item	Quantity	Unit Cost	Total Cost	Source	Part Number
Air Bushings 0.75 inch	4	\$331.00	\$1,324.00	New Way	S301201
Solenoid	1	\$64.94	\$64.94	McMasterCarr	7723K12
T-slot Framing 1 1/2 inch (96 inch length)	2	\$48.15	\$96.30	McMasterCarr	47065T119
T-slot Framing 1 1/2 inch (4 foot length for 6 inch braces)	1	\$25.15	\$25.15	McMasterCarr	47065T119
Incident & Transmission Bar: 1566 Steel Bar 0.75 inch (36inch length)	2	\$29.42	\$58.84	McMasterCarr	6061K64
Air Manifold (72 inches)	1	\$16.34	\$16.34	McMasterCarr	4457K35
T-slot Framing 1 1/2 inch (24 inch length) For stability	1	\$13.98	\$13.98	McMasterCarr	47065T119

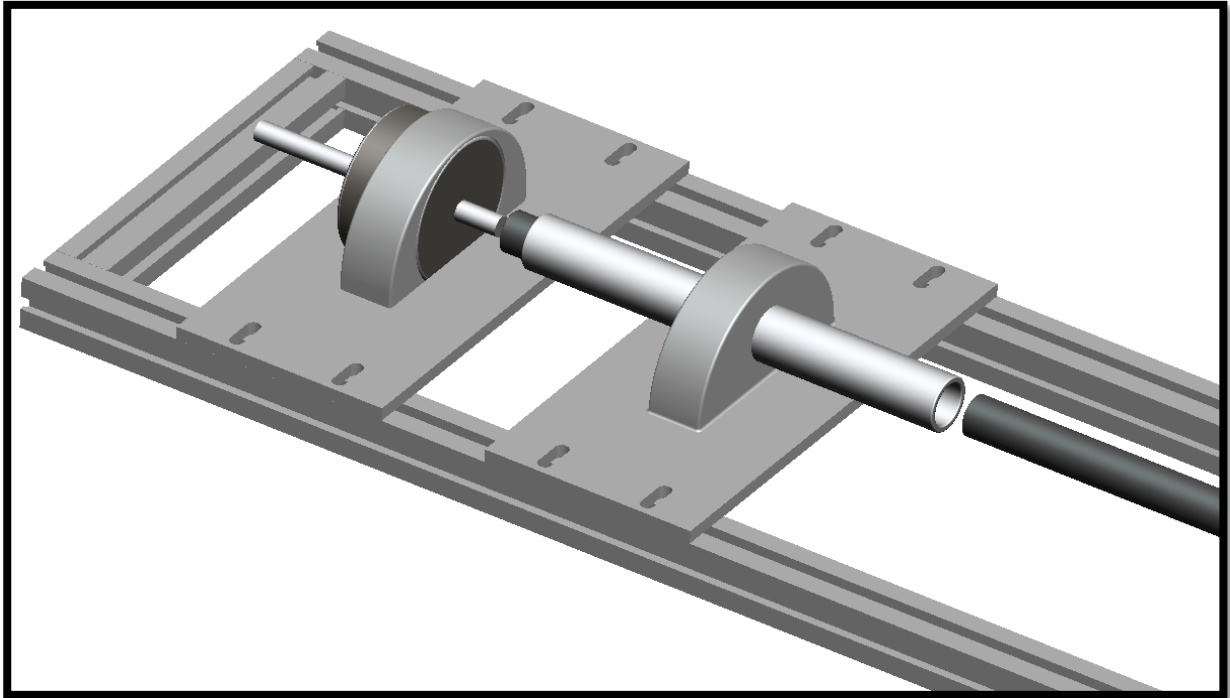
Striker Bar: 1566 Steel Bar 0.75 inch (12inch length)	1	\$10.25	\$10.25	McMasterCarr	6061K34
DAQ			\$0.00	COE	
Momentum Trap			\$0.00	Group	
Air supply			\$0.00	Group	

Pro Engineer Models -

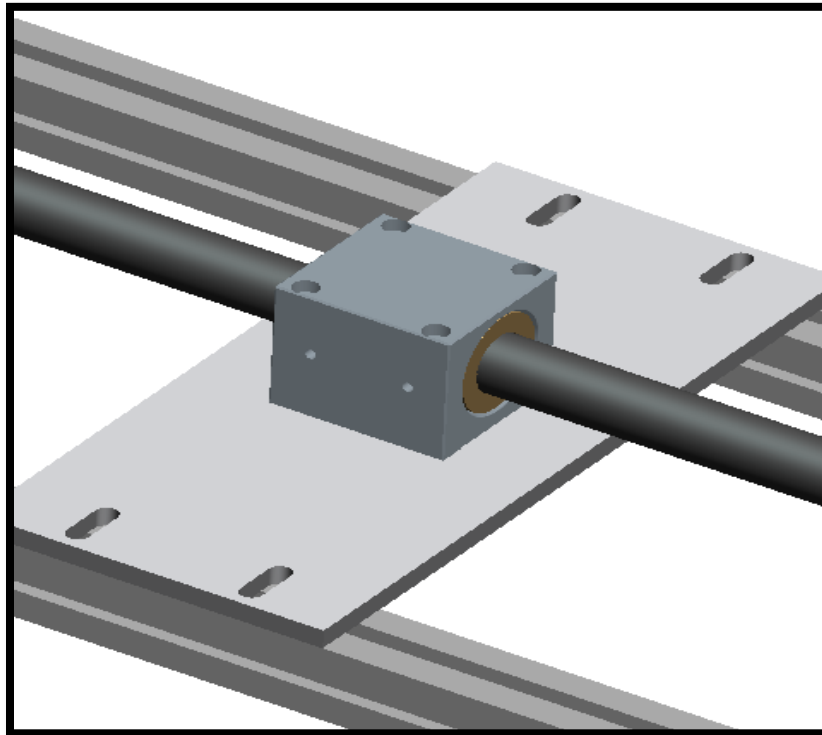
Final Design Overview



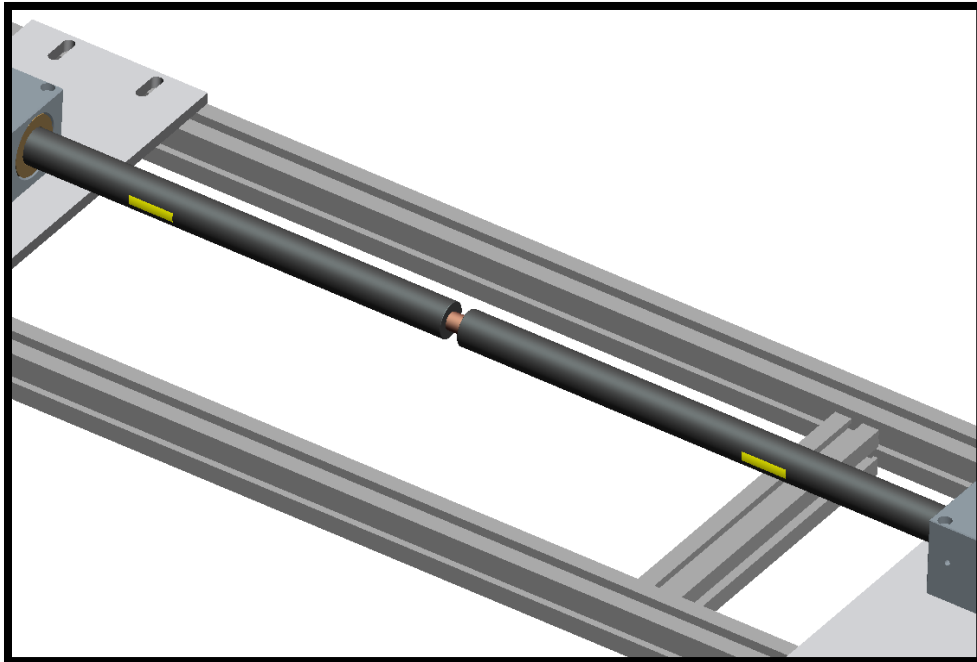
Striker bar mechanism



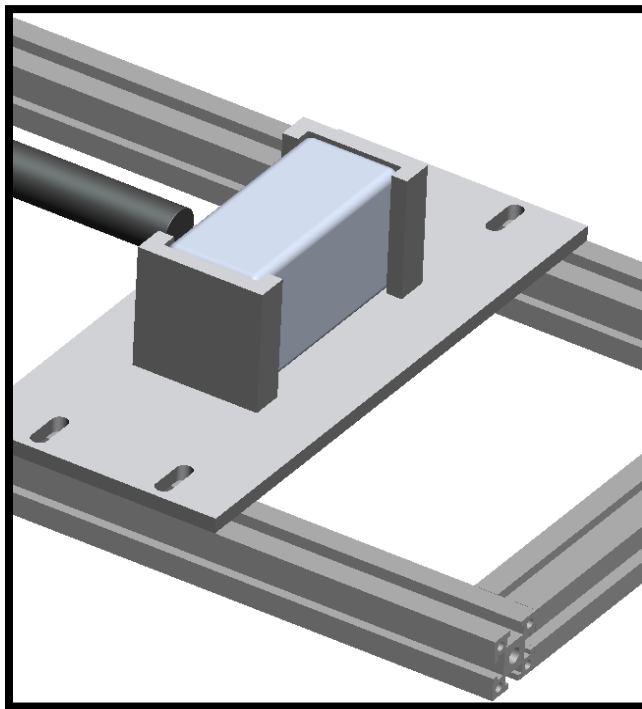
Bushing Block, Bushing, and Bar Installed



Bars, Sample, and Strain Gages



Momentum Trap



Pro-E drawing files and assemblies are available upon request.